Supercooled Water in PVA Matrixes. II. A Molecular Dynamics Simulation Study and Comparison with QENS Results

Ester Chiessi,* Francesca Cavalieri, and Gaio Paradossi

Dipartimento di Scienze e Tecnologie Chimiche, Università di Roma "Tor Vergata" and INFM, Via della Ricerca Scientifica, 00133, Roma, Italy

Received: November 12, 2004; In Final Form: February 23, 2005

Molecular dynamics (MD) simulations were carried out to elucidate the dynamic behavior of water confined in poly(vinyl alcohol), PVA, hydrogels. Model topology is supported by experimental network parameters, and simulation results are compared to an incoherent quasielastic neutron scattering (QENS) investigation carried out on PVA hydrogels.[1] From the QENS dynamic scattering law (part I),[1] a random jump model was adopted for the description of water diffusion to extract a microscopic diffusion coefficient and a residence time between two "jumps". In the present work, consistently with this framework, water diffusion parameters as diffusion coefficients and residence times have been evaluated using the mean square displacement of water in a time window of 10 ps and the time autocorrelation function of water hydrogen bonds. The calculated parameters are in good agreement with the experimental ones, giving confidence to this approach. Further developments are in progress to take into account a more realistic description of hydrogel structure in the molecular dynamics simulations.

1. Introduction

The macroscopic behavior of hydrogels has been studied since the beginning of macromolecular science,[2] yet only recently have the dynamic processes occurring within a hydrogel been a matter of investigation experimentally[1,3−6] as well as theoretically.[7,8] The availability of new experimental approaches probing distances and times on the molecular level provided by modern facilities as high-flux neutron sources and X-ray synchrotrons[9−11] has allowed detailed insight into this subject. The parallel development of computational methods applied to protein and other macromolecular species[12] has also triggered interest in the gel state. In this context, the study of water dynamics in hydrogels is part of an increasing number of investigations concerning the study of nonreactive processes in the wider class of systems where water is confined in cages with different chemical and structural features.[13−16]

Many experimental approaches are adopted in the study of macroscopic equilibrium and dynamic properties of hydrogel systems. Swelling and viscoelastic properties and the selective absorption of permeants provide information on structural features such as the mesh size and the average molecular weight of a strand between two cross links. Static and dynamic properties on the molecular scale can be investigated by scattering techniques, and in this context, incoherent quasielastic neutron scattering (QENS) is a powerful tool as exchanged energies activate rotational and translational motions, accessing space and time windows suitable for dynamic processes occurring in gels and amenable to simulation by means of modern molecular dynamics approaches.

Different types of chemical hydrogels based on poly(vinyl alcohol), PVA, have been prepared in our laboratory and characterized by several techniques.[1,6,17−18] In part I of this work, QENS spectroscopy has been used to understand the relationships occurring between the diffusional parameters of water and the polymer network architecture.[1] Solvent diffusion coefficients and residence times in these hydrophilic systems indicate that water behaves as a supercooled liquid phase. Moreover, a confined segmental motion of the polymer chains is observed.

Although the accomplishment of a completely satisfactory description of water is still matter of debate,[19−20] MD simulation represents an established tool in the investigation of biomacromolecular systems in an aqueous environment.[12,21] This technique has been applied to the study of confined water in hydrophobic/hydrophilic matrixes, such as Vycor glass,[22] carbon nanotubes,[23] zeolites,[24] clay,[25] vermiculite,[13] and cellular membrane channels.[26]

Quite surprisingly, MD studies of hydrogel systems are relatively scarce. Models of physical hydrogels (i.e., polymer networks where junction zones are stabilized by noncovalent bonds) have been investigated by MD simulations in the work of Tamai et al.[27−29] Poly(vinyl alcohol), poly(vinyl methyl ether), and poly(*N*-isopropylacrylamide) chains were modeled in water boxes for a maximum water content of about 80%. The authors focused on the hydrogen-bonded structure of the entangled chains and on their dynamics and on the diffusion behavior of water as well as of O_2 and N_2, treated as penetrants.[30]

Chemical polyacrylamide hydrogels have been simulated at high polymer concentrations (from 27 to 41 wt %) at temperatures ranging from 270.6 to 301.7 K.[8] A polymer-induced modification of solvent properties has been detected in the first hydration shell, resulting in an anisotropic spatial distribution of bound water around the matrix with a decreased diffusion coefficient and increased residence probability.

In recent work by Mijovic and Zhang,[31] the MD approach is applied to chemical epoxy-amine networks at very low degrees of hydration (0 to 8 wt %).

The present study reports on a molecular dynamics investigation of a PVA chemical hydrogel with the aim of exploring at

* Corresponding author. E-mail: ester.chiessi@uniroma2.it.

10.1021/jp044807f CCC: $30.25
Published on Web 04/05/2005

TABLE 1: Structural Parameters for PVA-Based Network from Dynamic-Mechanical Experiment

$\rho \times 10^5$ (mol·cm^{-3})	M_c (g·mol^{-1})	ξ (nm)
2.7	1054	4.6

CHART 1: PVA Junction Model

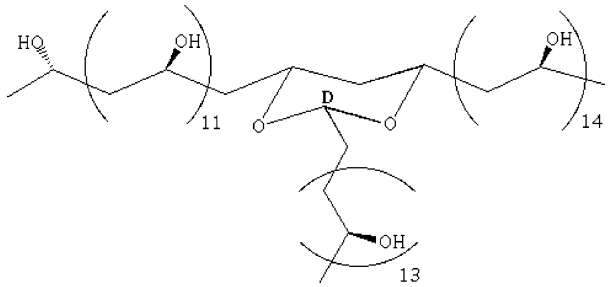

the molecular level the polymer-induced modification of water properties and comparing the theoretical results with the experimental findings obtained by the QENS study.[1] This work represents, to our knowledge, the first MD study of a chemical hydrogel under appropriate conditions for biomedical and pharmaceutical applications.[32,33] Parameters such as the polymer concentration (10% w/v), mesh size (about 4.6 nm), and linear mass density of the chains (about 7 residues/nm) have been chosen to be consistent with the experimental values. The solidlike nature of the macroscopic hydrogel has been replaced by constraining the position of the three most external carbon atoms of the matrix. The reported results provide a picture of the supercooled water embedding in the polymer, in good agreement with experimental findings obtained by QENS studies of the same system.[1]

2. Methods

2.1. Dynamic-Mechanical Experiment. Telechelic PVA hydrogels were prepared according to the procedure already published.[17] The viscoelastic properties of the hydrogel samples were tested by means of a dynamic-mechanical analysis (DMA) instrument working in compression mode (Perkin-Elmer DMA-7). Slabs of swollen telechelic PVA hydrogels were tested by applying a dynamic strain of 0.2% at a frequency of 1 Hz. The cross-link density, ρ, molecular weight between cross links, M_c, and average pore size, ξ, were determined from the linear region of the stress−strain curves on the basis of the Gaussian rubber elasticity theory.[2,34] The relevant parameters for developing a realistic representation of the hydrogel are listed in Table 1.

2.2. Developing the Model. The polymer network model developed for the simulation contains a three-functional junction zone shown in Chart 1.

In this representation, the network element is constituted of three atactic PVA linear chains, formed by 11, 14, and 13 repeating units connected by a 1,3-dioxane cyclic residue. The chosen polymer lengths were dictated by the mesh size and polymer chain density according to the parameters reported in Table 1. Only head-to-tail sequences have been assumed for the PVA description because the head-to-head linkages, present in a few percent in PVA samples, are oxidized during the synthesis of the chemical hydrogel.[17] The GROMACS force field with the united atom convention for CH and CH_2 groups was used; preliminary minimizations and dynamics, as well as the production MD simulations, were carried out by GROMACS software, version 3.1.4.[35,36] The force-field parameters are quite similar to those previously used in reported studies of PVA aqueous solutions.[37,38] The 1,3-dioxane six-membered ring has been treated as a nonreducing glucose residue, assuming a chair conformation and equatorial configuration of the three carbon atoms linked to the chains; see Chart 1.

CHART 2: Two-Dimensional Projection of the Simulated PVA Network[a]

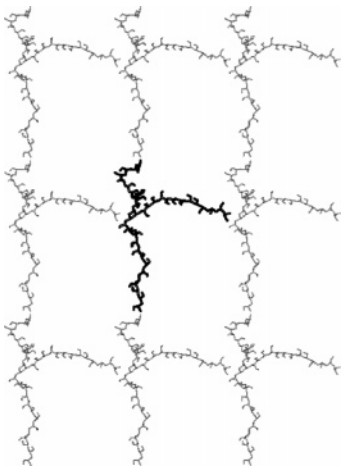

[a] Junction model (bold) and periodic replicas.

Starting with the three PVA segments in an all-trans conformation, a preliminary energy minimization (steepest descent) and 20 000 steps dynamics in vacuo at 300 K, with time step of 0.5 fs, were carried out to obtain a more realistic sampling of the conformational space. In this calculation, all of the electrostatic interactions were turned off. From the analysis of the last 2 ps of the trajectory, a structure has been selected on the basis of the best agreement with the experimental average linear mass density of 7 residue/nm, treating the mesh as a square and assuming the mesh size to be equal to its diagonal.

The PVA structure has then been hydrated in a cubic box with 4 nm sides. Water has been simulated by the single-point charged (SPC) intermolecular potential model.[39] A steepest-descent energy minimization and 450 ps of molecular dynamics have been calculated at 303 K on the PVA in the water cubic box. (See section 2.3.)

At this stage, the polymer has been assumed to be conformationally relaxed. The modeled junction structure described in the last frame has been oriented in a new orthorhombic simulation box sized to match the polymer chain length and chain density and to mimic the network topology, as sketched in Chart 2.

A harmonic position restraint potential has been applied to the terminal CH_2 group of each linear chain to remove the translational and rotational degrees of freedom of the network and to maintain covalent bond distances between the modeled PVA network element and its periodic images. The orthorhombic box contained 1063 SPC water molecules. With this setting, a cross-link density of 5×10^{-5} mol/cm^3 has been obtained. A further steepest-descent energy minimization has been carried out, and the system has been used as a starting model for the MD study.

2.3. Simulation Details. Calculations have been performed on the SP4 IBM computer of the CINECA Supercomputing Center (Bologna, Italy).

All MD simulations have been carried out in the NVT ensemble, with the leap-frog integration algorithm[40] using a time step of 0.5 fs, periodic boundary conditions, and the minimum image convention. Temperature has been controlled by the Berendsen's coupling algorithm with a time constant equal to

the time step to approximate the Gaussian isokinetic thermostat.[41,42] Long-range electrostatic interactions have been calculated using the particle-mesh Ewald method and applying a cutoff of 0.9 nm to the short-range Lennard-Jones interactions. The SETTLE algorithm[43] is used to fix the water molecule geometry, and the SHAKE algorithm,[44] to constrain the O−H distance in the PVA hydroxylic groups. The temperatures considered (291, 303, 313, and 323 K) have been chosen according to the QENS experiments.[1] The total simulation time, including equilibration and production run, was 1.1 ns at 291 K, 700 ps at 303 K, 600 ps at 313, and 600 ps at 323 K. The last 400 ps trajectory has been used for analysis at each temperature. The configurations were saved every 0.1 ps.

MD simulations have also been performed for pure water in the same simulation box of the hydrogel containing 1142 water molecules. The total simulation time was 200 ps at each temperature, and the last 100 ps trajectory has been considered for analysis.

2.4. Analysis Procedures. The hydrogen bond occurrence between a hydrogen donor atom D and an acceptor atom A was evaluated using the following geometric criteria: $R(\mathrm{H}\cdots\mathrm{A}) < 0.25$ nm and $\theta(\mathrm{D}-\mathrm{H}\cdots\mathrm{A}) < 60°$, where $R(\mathrm{H}\cdots\mathrm{A})$ is the distance between hydrogen and the acceptor atom and $\theta(\mathrm{D}-\mathrm{H}\cdots\mathrm{A})$ is the angle formed by the three atoms (a linear arrangement results for $\theta = 0$).

The dynamics of hydrogen bonds, HB, was evaluated by studying the normalized time autocorrelation function

$$C_{\mathrm{HB}}(t) = \frac{\langle s_{ij}(t_0)\, s_{ij}(t + t_0)\rangle}{\langle s_{ij}(t_0)\, s_{ij}(t_0)\rangle} \qquad (1)$$

where the state variable s_{ij} has a value of 1 or 0 depending on the existence or nonexistence of an HB between a selected donor−acceptor pair ij. t_0 and t in eq 1 range from 0 to half of the simulation time considered for analysis. The function $s_{ij}(t + t_0)$ is set to 1 if the HB between ij is found to be present in the time steps t_0 and $t_0 + t$, even if the same HB can be interrupted at some intermediate time. According to the given definition, the $C_{\mathrm{HB}}(t)$ function reflects the effective time persistence of a hydrogen bond, allowing the comparison of the HB correlation time with the QENS residence time and taking into account that breaking an HB can also occur as a consequence of the loss of the orientational requirements regardless of translational process (i.e., diffusion). The correlation time, τ, has been obtained by integrating $C_{\mathrm{HB}}(t)$ in a time window of about 10τ because the time autocorrelation functions shows nonexponential behavior for both the model hydrogel and the bulk water, as already found in other simulation studies.[45]

Usually the analysis of the structural dynamic factor obtained from QENS measurements according to the random jump diffusion model[46] supplies information about the diffusional processes in the hydrogel in terms of a characteristic residence time in one configuration site and a microscopic diffusion coefficient. These parameters can be related in the simulation to the average characteristic lifetime of the HB correlation function, eq 1, and the diffusion coefficient calculated from the long-time slope of the mean square displacement, eq 2

$$D = \frac{1}{6}\lim_{t\to\infty}\frac{\mathrm{d}}{\mathrm{d}t}\langle|\mathbf{r}(t) - \mathbf{r}(0)|^2\rangle \qquad (2)$$

where $\mathbf{r}(t)$ and $\mathbf{r}(0)$ correspond to the position vector of the water oxygen at time t and 0, respectively, with an average performed over both time origins and water molecules.

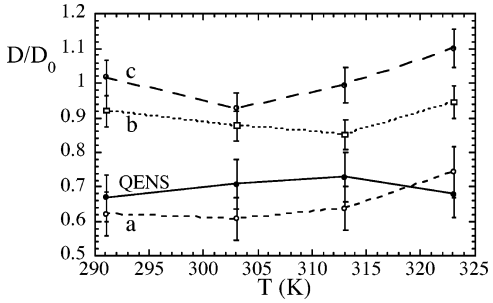

Figure 1. Ratio between diffusion coefficient of water molecules of different domains in the hydrogel, D, and diffusion coefficient of water bulk, D_0, as a function of temperature. (a) Water molecules in the first hydration shell; (b) water molecules with a distance from PVA between 0.336 and 0.8 nm; (c) water molecules with a distance from PVA larger than 0.8 nm. D_0 is the value calculated from MD simulations of bulk water. QENS: experimental diffusion coefficients,[1] normalized to the diffusion coefficient of bulk water.[48]

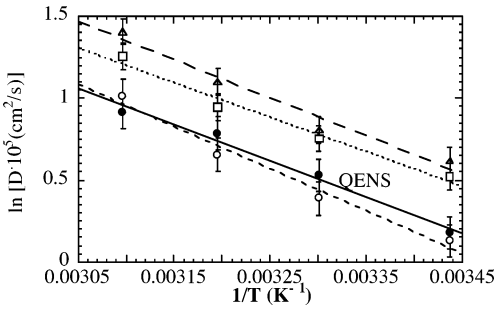

Figure 2. Arrhenius plots of water diffusion coefficients. Calculated values for a (○), b (□), and c (△) domains of water molecules (see text). QENS: experimental values (●).

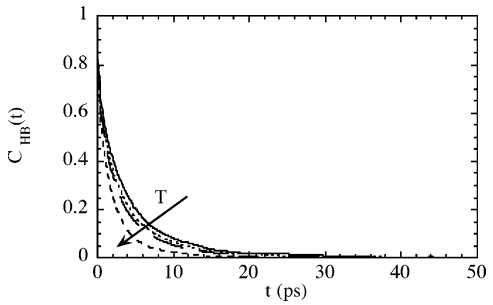

Figure 3. Decay of the water HB autocorrelation function $C_{\mathrm{HB}}(t)$ for different temperatures {(—) 291 K; (- - -) 303 K; (— —) 313 K; and (— —) 323 K} within a region of 0.8 nm from the carbon atom labeled D in Chart 1.

For the analysis of the diffusion coefficients, water molecules were geometrically classified in three domains according to defined distance thresholds from the polymer chain. The first one accounts for the first hydration shell and includes water molecules within a distance of 0.336 nm from the polymer, corresponding to the first minimum of the radial distribution function between PVA oxygen and water oxygen (Figure 4a). The second domain includes water molecules in a shell between 0.336 and 0.8 nm, whereas the third one contains the remaining water molecules in the simulation box. A time window of 10 ps corresponding to the correlation time of the HB autocorrelation function between PVA and water is chosen for the calculation of the average diffusion coefficient of the water molecules inside each domain. In this representation, a loss of correlation indicates the leaving of a water molecule from the polymer matrix. Therefore, a 10 ps correlation time represents the average residence time of water molecules in the polymer hydration shell.

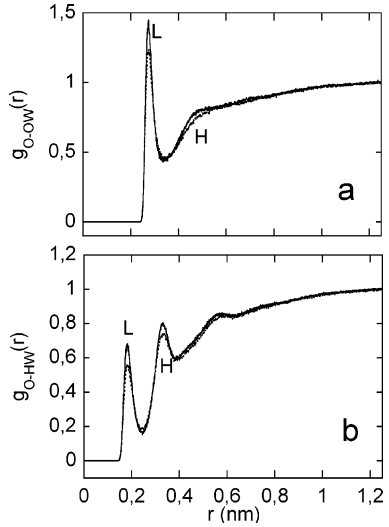

Figure 4. Radial distribution functions of PVA oxygens with water oxygens (a) or water hydrogens (b) at 291 K (curves L) and 323 K (curves H).

With the aim of evaluating the confidence interval of the results, the diffusion coefficient was calculated every 50 ps for the last 400 ps trajectory.

3. Results and Discussion

3.1. Water Dynamics. The QENS study of PVA hydrogels provided information about the solvent diffusion using the unrestricted jump model of Singwi and Sjölander.[46] According to this description, water molecule displacements are described in terms of a random walk, and the time needed for moving from one site to another, usually indicated as a jump, is negligible with respect to the residence time in a single site. The solvent mobility is treated in terms of the microscopic diffusion coefficient, the residence time, and the mean square length of a jump. As was shown for different types of hydrogels,[6,47] QENS spectra probe two water ensembles with different diffusive properties, namely, a "slow" and a "fast" fraction of diffusing solvent molecules. The slowly relaxing fraction of water displays behavior similar to supercooling, a typical effect in confining matrixes.[1,6,47]

In MD trajectories, water molecules have been geometrically classified in three groups as previously described in section 2.4. The simulation results show that in the first hydration shell of the polymer, labeled as group a, about 100 water molecules are present, whereas in the domain between 0.336 and 0.8 nm, 450 molecules were contained, indicated as group b. Group c occupying the remaining box space consists of about 500 molecules. As the next step, the average diffusion coefficient of water molecules belonging to each domain has been calculated as the long-time limiting slope of the mean square displacement, according to eq 2. In the comparison between QENS and MD values of diffusion coefficients of water, shown in Figure 1, results have been normalized to the diffusion coefficient of bulk water, $D_0(T)$ at the corresponding temperature, to cancel out artifacts residing in the SPC potential model.

Group a and, to a minor extent, also the water of group b show a diffusion coefficient lower than that of group c, which has values of D/D_0 approaching unity and indicating, for this last group of water molecules at a distance larger than 0.8 nm, dynamic behavior analogous to that of bulk water. The diffusion behavior of the slow water fraction, in terms of D/D_0, observed in the QENS investigation compares favorably, within the approximations of the methods, with the calculated diffusion coefficient ratio of the first hydration shell of water molecules, as shown in Figure 1. The confinement effect on water is reflected by the extent of the D/D_0 decrease, relating the diffusion coefficient parameter to the distance from PVA. A comparison of b- and c-type diffusion with experiment is not possible for this system because the QENS study provided information only on the dynamics of the bound water of the first shell of hydration, whereas the fast-relaxing water component was not accurately characterized experimentally.

The temperature independence of the D/D_0 ratio for both the observed values and the calculated ones indicates an almost equivalent activation energy of water diffusion in the hydrogel and bulk.

The Arrhenius plots based on the diffusion coefficients, shown in Figure 2, provide the same activation energy of 4.5 ± 0.5 kcal/mol in the temperature range from 291 to 323 K irrespective of the water domains and compared reasonably well with the experimental value of 4.0 ± 0.6 kcal/mol obtained in the QENS study.[1]

Chemical or physical hydrogels present at the microscopic level structural and dynamic heterogeneities.[49] In the proximity of the junctions of the network, higher polymer concentrations and topological constraints influence the dynamic properties of both the matrix and water. In this respect, simulations of network models can give insight into the gel state that is otherwise experimentally difficult to access. Toward this aim, we have analyzed the MD trajectories focusing on the water molecule dynamics in the surroundings of the junction node contained in the model. For the study of the hydrogen bonding of water involved in the solvation of this part of the network, we have included in the analysis the solvent molecules contained in a sphere with a radius of 0.8 nm measured from the carbon atom of the 1,3-dioxane residue labeled D in Chart 1. A cutoff of 0.8 nm has been chosen as the distance where spatial correlation between the D atom and the oxygen atoms of the surrounding water molecules is completely lost, according to the corresponding radial distribution function (section 3.2). The resulting time correlation functions are shown in Figure 3 for the investigated temperatures.

The same approach has been carried out considering as the central atom of the sphere an oxygen placed on one of the polymer chains constituting a branch of the network model. For the sake of comparison, we performed the same analysis on an equivalent spherical domain in a simulation box containing only bulk water.

The relaxation behavior of water molecule HBs in regions centered on different positions of the model network is reported in Table 2.

A general increase in the HB lifetimes with respect to the value of the bulk, τ_{bulk}, is found. A longer lifetime is observed when the calculation is carried out in the region centered on carbon atom D (Chart 1). The HB lifetime of water molecules probed in the region centered on a polymer branch, τ_{chain}, is

TABLE 2: Water Hydrogen Bond Lifetimes in Different Domains of PVA Hydrogel

T (K)	τ_D (ps)[a]	τ_{chain} (ps)[b]	τ_{bulk} (ps)[c]	τ_{QENS} (ps)[d]
291	3.6 ± 0.4	2.7 ± 0.2	2.1 ± 0.1	3.3 ± 0.3
303	3.0 ± 0.2	2.4 ± 0.1	1.5 ± 0.1	3.0 ± 0.3
313	2.5 ± 0.2	1.9 ± 0.1	1.3 ± 0.1	2.8 ± 0.3
323	1.9 ± 0.1	1.6 ± 0.1	1.2 ± 0.1	2.4 ± 0.2

[a] Water domain with a radius of 0.8 nm from atom D (Chart 1). [b] Water domain with a radius of 0.8 nm from a PVA chain. [c] Bulk water. [d] Experimental QENS values of the residence time.

TABLE 3: Solvation Features of PVA Matrix

T (K)	R_{min} (nm) in eq 3	average coordination number of PVA oxygen, n_{O-OW}
291	0.336 ± 0.002	2.08 ± 0.04
303	0.340 ± 0.002	2.12 ± 0.04
313	0.347 ± 0.002	2.23 ± 0.04
323	0.348 ± 0.002	2.28 ± 0.05

intermediate between τ_D and τ_{bulk}. Simulated HB lifetimes τ_D are in good agreement with the experimental residence time, τ_{QENS}, at all explored temperatures, except for the value at 323 K. This discrepancy is presently under study.

The total average number of hydrogen bonds per water molecule, counting both polymer−water and water−water interactions, is 1.6 in the region including the junction compared to a value of 1.4 found in the simulation of the bulk. This feature, obtained from the simulation study of the system, is in agreement with the picture of supercooled water behavior derived from the QENS experiment.

3.2. Polymer−Water Interaction. The solvation of the polymer moiety has been analyzed in terms of radial distribution functions between oxygen of PVA and oxygen or hydrogen of water $g_{O-OW}(r)$ and $g_{O-HW}(r)$, respectively. These distribution functions refer to the probability of finding the water oxygen atom or a water hydrogen atom at a distance r from the oxygen atom of PVA.

The $g_{O-OW}(r)$ and $g_{O-HW}(r)$ at 291 K (curves L) and at 323 K (curves H) are shown in Figure 4a and b, respectively.

A temperature increase causes a mild destructuring of water molecules in the first hydration shell, as is indicated by the maxima and minima attenuations in both distribution functions, whereas their positions remain unchanged by temperature variations. The maximum position in Figure 4a, representing the most probable configuration between PVA and water oxygen atoms, is at 0.28 nm, in agreement with a hydrogen bond regime in the first solvation shell of PVA. The number of water molecules in this domain can be evaluated by integration of $g_{O-OW}(r)$ according to eq 3

$$n_{O-OW}(R_{min}) = \frac{N_{OW}}{V}\int_0^{R_{min}} 4\pi r^2\, g_{O-OW}(r)\, dr \qquad (3)$$

where N_{OW}, V, and R_{min} are the total number of water molecules in the box, the volume of the simulation box, and the distance of the first minimum of $g_{O-OW}(r)$, respectively. The temperature dependence of R_{min} and n_{O-OW} is reported in Table 3.

An average coordination number of 2.2 water molecules per PVA oxygen is obtained in agreement with findings from MD studies of PVA solutions[37] and physical hydrogels.[27]

Integration of the radial distribution function $g_{O-HW}(r)$ shown in Figure 4b is carried out according to eq 4

$$n_{O-HW}(R_{min}) = \frac{N_{HW}}{V}\int_0^{R_{min}} 4\pi r^2\, g_{O-HW}(r)\, dr \qquad (4)$$

where N_{HW} corresponds to the total number of hydrogen water atoms in the system. The integral yields the average number of water hydrogen atoms coordinating a PVA oxygen atom, n_{ACC}, and represents an estimate of the average number of hydrogen bonds per PVA oxygen acting as acceptors (second column of Table 4). The total average number of hydrogen bonds per PVA oxygen (both as a donor and acceptor), n_{TOT}, has been obtained by direct analysis of the trajectories, seeking the occurrence of PVA−water HBs in the collected frames according to the geometric criteria discussed in section 2.4. The average number

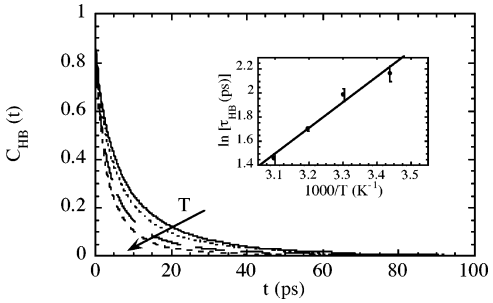

Figure 5. HB autocorrelation function $C_{HB}(t)$ between PVA hydroxylic groups and water for different temperatures: (—) 291 K; (- - -) 303 K; (— —) 313 K; and (— — —) 323 K. Inset: Arrhenius plot of the HB lifetime, τ, calculated as the integral of $C_{HB}(t)$ from 0 to 100 ps.

TABLE 4: Features of Hydrogen Bond between PVA and Water

T (K)	n_{ACC}	n_{TOT}	n_{DO}	n_{ACC}/n_{DO}	HB lifetime (ps)
291	0.94 ± 0.02	1.69 ± 0.09	0.75 ± 0.11	1.2 ± 0.2	8.7 ± 0.6
303	0.93 ± 0.02	1.67 ± 0.12	0.74 ± 0.14	1.3 ± 0.2	7.3 ± 0.4
313	0.91 ± 0.02	1.60 ± 0.09	0.69 ± 0.11	1.3 ± 0.2	5.5 ± 0.1
323	0.85 ± 0.02	1.57 ± 0.12	0.72 ± 0.14	1.2 ± 0.2	4.3 ± 0.2

of hydrogen bonds per PVA oxygen acting only as a donor, n_{DO}, is the difference between the total number and the number of HBs acting as an acceptor. Alternatively, the same parameter can be evaluated by integrating the pair correlation function between polymer hydrogens and water oxygens (i.e., $g_{H-OW}(r)$) similarly to eq 3 or 4. Results obtained by these two procedures are in agreement within the errors.

From an inspection of Table 4, it can be noted that the ratio between the values of the second and fourth columns, n_{ACC}/n_{DO}, is less than 2. A ratio of 2 would reflect the capacity of PVA hydroxyl groups to form HBs as a donor or acceptor indifferently because of the presence of two oxygen lone pairs and one hydrogen atom. In our case, the obtained ratios are about 1.3 for all temperatures, indicating that PVA hydroxyl groups act preferentially as a donor.

Values of n_{TOT} in Table 4 indicate the good accessibility of the solvent to the hydrophilic groups of the polymer matrix and, in the explored temperature range, a decreasing trend in the number of PVA−water hydrogen bonds with increasing temperature.

Also in the case of interaction between the polymer moiety and water, the hydrogen bond dynamics was analyzed using the time autocorrelation function, $C_{HB}(t)$, defined by eq 1. Figure 5 shows the autocorrelation functions for the PVA−water hydrogen bonds at different temperatures calculated from the last 200 ps trajectories. The autocorrelation functions are nonexponential, and their correlation times, τ_{HB}, at different temperatures have been evaluated by integration of $C_{HB}(t)$ and reported in Table 4. The corresponding Arrhenius plot (inset of Figure 5) yields an activation energy of 3.8 ± 0.5 kcal/mol, typical of hydrogen bond rearrangements.

The number of water molecules in direct interaction with PVA has been calculated for each saved frame. At 303 K, the results supply a picture of the dynamics occurring in the solvation of PVA, where a time-averaged set of 69 water molecules directly involved in hydrogen bonding with PVA, out of a total of 1063 water molecules, are completely replaced in about 7 ps.

As far as the dynamics of the polymer network is concerned, the results of QENS measurements on PVA hydrogels, carried out by replacing water with D_2O to rule out the solvent contribution to the overall scattering, indicate a regime of

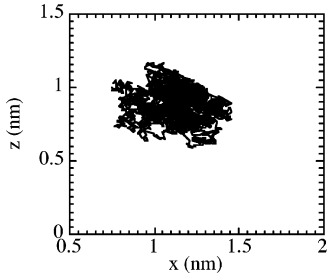

Figure 6. Trace of atom D of PVA at 323 K. Projection into the *xz* plane.

constrained diffusion, with an average displacement of about 0.9 nm, according to the diffusion between two impenetrable walls (Ross and Hall).[50] From this analysis, a few hundreds of picoseconds is estimated to be the characteristic time scale on which polymer segmental motions occur. An activation energy of about 4 kcal/mol, related to the transition between segmental conformations, has been determined by the Arrhenius analysis of the characteristic times.[1]

The 400 ps trajectory at 323 K of atom D (Chart 1), representing the junction mobility, projected on the *xz* plane is shown in Figure 6. The extent of explored space, about 0.8 nm on average, is in agreement with the QENS results.

4. Concluding Remarks

The present molecular dynamics study of a PVA chemical hydrogel has focused on the influence of the polymer confinement on the water dynamic behavior in terms of diffusional properties and hydrogen bond interactions. A supercooling effect on water has been found in agreement with experimental results of a QENS study performed on a PVA hydrogel. According to MD calculations, this finding concerns a water domain centered around the polymer with a thickness of about 0.8 nm. In this region, the solvent dynamics is slowed by HB interaction with the hydroxylic groups of the PVA chain, and the activation barriers relative to the diffusion coefficients and residence times are typical of hydrogen bond interactions.

The diffusion parameters derived from the simulations and concerning the first hydration shell compare favorably with the QENS findings as well as their temperature dependence. A simplified model of a hydrated network has been used for the description of a PVA hydrogel, providing a picture closely resembling the dynamic behavior of the polymer moiety and of water. In particular, the model has showed the importance of the junction zone domains in determining the overall dynamic properties of the solvent. Future extensions to higher periodicity models are in progress to include long-range effects involving the polymer chains that can account for gel state features such as responsivity to pH and temperature.

Acknowledgment. We gratefully acknowledge Professor G. B. Suffritti for helpful discussions, Mr. A. Scagliarini for carrying out some preliminary simulations, and INSTM/CINECA for partial financial support.

References and Notes

(1) Paradossi, G.; Cavalieri, F.; Chiessi, E.; Telling, M. T. F. *J. Phys. Chem. B* **2003**, *107*, 8363.

(2) Flory, P. J. *Principles of Polymer Chemistry*; Cornell University Press: Ithaca, NY, 1953.

(3) McConville, P.; Whittaker, M. K.; Pope, J. M. *Macromolecules* **2002**, *35*, 6961.

(4) Di Bari, M.; Cavatorta, F.; Deriu, A.; Albanese, G. *Biophys. J.* **2001**, *81*, 1190.

(5) Ruffle, S. V.; Michalarias, I.; Li, J.; Ford, R. C. *J. Am. Chem. Soc.* **2002**, *124*, 565.

(6) Paradossi, G.; Di Bari, M. T.; F.; Telling, M. T. F.; Turtu', A.; Cavalieri, F. *Physica B* **2001**, *301*, 150.

(7) Fernandes, M. X.; Garcia de la Torre, J.; Castanho, M. A. R. B. *J. Phys. Chem. B* **2000**, *104*, 11579.

(8) Netz, P. A.; Dorfmüller, T. *J. Phys. Chem. B* **1998**, *102*, 4875.

(9) Gabel, F.; Bicout, D.; Lehnert, U.; Tehei, M.; Weik, M.; Zaccai, G. *Q. Rev. Biophys.* **2002**, *35*, 327.

(10) Winter; R. *Biochim. Biophys. Acta* **2002**, *1595(1−2)*, 160.

(11) Koch, M. H.; Vachette, P.; Svergun, D. I. *Q. Rev. Biophys.* **2003**, *36*, 147.

(12) Hansson, T.; Oostenbrink, C.; van Gunsteren, W. F. *Curr. Opin. Struct. Biol.* **2002**, *12*, 190.

(13) Bergman, R.; Swenson, J. *Nature* **2000**, *403*, 283.

(14) Crupi, V.; Majolino, D.; Migliardo, P. Venuti, V. *J. Phys. Chem. A* **2000**, *104*, 11000.

(15) Pal, S.; Balasubraminian, S.; Bagchi, B. *Phys. Rev. E* **2003**, 061502.

(16) Dore, J. *Chem. Phys.* **2000**, *258*, 327.

(17) Paradossi, G.; Cavalieri, F.; Capitani, D.; Crescenzi, V. *J. Polym. Sci., Part B: Polym. Phys.* **1999**, *37*, 1225.

(18) Barretta, P.; Bordi, F.; Rinaldi, C.; Paradossi, G. *J. Phys. Chem. B* **2000**, *104*, 11019.

(19) Yu, H.; Hansson, T.; van Gunsteren, W. F. *J. Chem. Phys.* **2003**, *118*, 221.

(20) van Maaren, P. J.; van der Spoel, D. *J. Phys. Chem. B* **2001**, *105*, 2618.

(21) Bizzarri, A. R.; Cannistraro, S. *J. Phys. Chem. B* **2002**, *106*, 6617.

(22) Gallo, P.; Rovere, M.; Spohr, E. *J. Chem. Phys.* **2000**, *113*, 11324.

(23) Hummer, G.; Rasaiah, J. C.; Noworyta, J. P. *Nature* **2001**, *414*, 188.

(24) Cicu, P.; Demontis, P.; Spanu, S.; Suffritti, G. B.; Tilocca, A. *J. Chem. Phys.* **2000**, *112*, 8267.

(25) Swenson, J.; Bergman, R.; Longeville, S.; Howells, W. S. *Physica B* **2001**, *301*, 28.

(26) Fujiyoshi, Y.; Mitsuoka, K.; de Groot, B. L.; Philippsen, A.; Grubmüller, H.; Agre, P.; Engel, A. *Curr. Opin. Struct. Biol.* **2002**, *12*, 509.

(27) Tamai, Y.; Tanaka, H.; Nakanishi, K. *Macromolecules* **1996**, *29*, 6750.

(28) Tamai, Y.; Tanaka, H.; Nakanishi, K. *Macromolecules* **1996**, *29*, 6761.

(29) Tamai, Y.; Tanaka, H. *Chem. Phys. Lett.* **1998**, *285*, 127.

(30) Tamai, Y.; Tanaka, H. *Fluid Phase Equilib.* **1998**, *144*, 441.

(31) Mijovic, J.; Zhang, H. *J. Phys. Chem. B* **2004**, *108*, 2557.

(32) Langer, R.; Tirrel, D. A. *Nature* **2004**, *428*, 487.

(33) Hoffman, A. S. *Adv. Drug Delivery Rev.* **2002**, *54*, 3.

(34) Peppas, N. A.; Barr-Howell, B. D. In *Hydrogels in Medicine and Pharmacy*; Peppas, N. A., Ed.; CRC Press: Boca Raton FL, 1986; Chapter 2.

(35) Berendsen, H. J. C.; van der Spoel, D.; van Drunen, R. *Comput. Phys. Commun.* **1995**, *91*, 43.

(36) Lindahl, E.; Hess, B.; van der Spoel, D. *J. Mol. Model.* **2001**, *7*, 306.

(37) Müller-Plathe, F.; van Gunsteren, W. F. *Polymer* **1997**, *38*, 2259.

(38) Müller-Plathe, F. *J. Membr. Sci.* **1998**, *141*, 147.

(39) Berendsen, H. J. C.; Postma, J. P. M.; van Gunsteren, W. F.; Hermans, J., In *Intermolecular Forces*; Pullman, B., Ed.; Reidel: Dordrecht, The Netherlands, 1981; p 239.

(40) Hockney, R. W.; Goel, S. P. *J. Comput. Phys.* **1974**, *14*, 148.

(41) Amadei, A.; Chillemi, G.; Ceruso, M. A.; Grottesi, A.; Di Nola, A. *J. Chem. Phys.* **2000**, *112*, 9.

(42) D'Alessandro, M.; Tenenbaum, A.; Amadei, A. *J. Phys. Chem. B* **2002**, *106*, 5050.

(43) Miyamoto, S.; Kollman, P. A. *J. Comput. Chem.* **1992**, *13*, 952.

(44) Ryckaert, J. P.; Ciccotti, G.; Berendsen, H. J. C. *J. Comput. Phys.* **1977**, *23*, 327.

(45) Luzar, A.; Chandler, D. *Nature* **1996**, *379*, 55.

(46) Singwi, K. S.; Sjölander, A. *Phys. Rev.* **1960**, *119*, 863.

(47) Cavatorta, F.; Deriu, A.; Di Cola, D.; Middendorf, H. D. *J. Phys. Condens. Matter* **1994**, *6*, A113.

(48) Krynicki, K.; Green, C. D.; Sawyer, D. W. *Faraday Discuss. Chem. Soc.* **1978**, 199.

(49) Shibayama, M. *Macromol. Chem. Phys.* **1998**, *199*, 1.

(50) Ross, D. K.; Hall, P. L. *Mol. Phys.* **1981**, 42, 673.